LightForce Photon-Pressure Collision Avoidance: Updated Efficiency Analysis Utilizing a Highly Parallel Simulation Approach

Jan Stupl, Nicolas Faber, Cyrus Foster
SGT Inc. / NASA Ames Research Center
Fan Yang Yang
Science and Technology Corporation / NASA Ames Research Center
Bron Nelson
Computer Science Cooperation / NASA Ames Research Center
Jonathan Aziz
University of Colorado, Boulder / NASA Ames Research Center
Andrew Nuttall
Stanford University
Chris Henze, Creon Levit
NASA Ames Research Center

ABSTRACT

This paper provides an updated efficiency analysis of the LightForce space debris collision avoidance scheme. LightForce aims to prevent collisions on warning by utilizing photon pressure from ground based, commercial off the shelf lasers. Past research has shown that a few ground-based systems consisting of 10 kW class lasers directed by 1.5 m telescopes with adaptive optics could lower the expected number of collisions in Low Earth Orbit (LEO) by an order of magnitude. Our simulation approach utilizes the entire Two Line Element (TLE) catalogue in LEO for a given day as initial input. Least-squares fitting of a TLE time series is used for an improved orbit estimate. We then calculate the probability of collision for all LEO objects in the catalogue for a time step of the simulation. The conjunctions that exceed a threshold probability of collision are then engaged by a simulated network of laser ground stations. After those engagements, the perturbed orbits are used to re-assess the probability of collision and evaluate the efficiency of the system. This paper describes new simulations with three updated aspects: 1) By utilizing a highly parallel simulation approach employing hundreds of processors, we have extended our analysis to a much broader dataset. The simulation time is extended to one year. 2) We analyze not only the efficiency of LightForce on conjunctions that naturally occur, but also take into account conjunctions caused by orbit perturbations due to LightForce engagements. 3) We use a new simulation approach that is regularly updating the LightForce engagement strategy, as it would be during actual operations. In this paper we present our simulation approach to parallelize the efficiency analysis, its computational performance and the resulting expected efficiency of the LightForce collision avoidance system. Results indicate that utilizing a network of four LightForce stations with 20 kW lasers, 85% of all conjunctions with a probability of collision $P_c > 10^{-6}$ can be mitigated.

1. INTRODUCTION

This paper presents an updated assessment of the efficiency analysis of the LightForce space debris collision avoidance concept that was presented at AMOS 2013 [25]. Last year's dataset was broadened significantly by extending the simulation time frame from 30 days to one year. This was enabled by porting the simulation to the Pleiades supercomputer at NASA Ames Research Center, a massively parallel multiprocessor system that utilizes up to 184,800 processor cores. The current assessment still uses the publicly available orbital data of all tracked space objects to create a baseline input for the simulations, providing a representative simulation of the space environment. In the previous paper, we assessed LightForce's effect on each conjunction (a conjunction is close approach between two objects), without taking effects of the induced orbit change on collision probability with third objects into account. We now continuously examine the whole environment and detect all conjunctions, whether they occur naturally or are an effect of changes introduced by Lightforce. We still use metrics based on probability of collision (PoC) between objects to assess the efficiency of the scheme.

The LightForce concept envisions reducing the risk of collisions by slightly changing the orbits of objects that are predicted to have a conjunction. Slight orbital perturbations are induced by photon pressure from ground-based,

industrial strength lasers (fig. 1). Earlier publications have introduced the concept and demonstrated the general viability of the scheme for a significant fraction of conjunctions [1, 2, 3], and last year's paper quantified the efficiency [25]. Based on a 30 day dataset, it was shown that even a limited number of stations could have a significant impact on the expected number of collisions, reducing it by an order of magnitude. This paper refines that assessment.

In the past, the space debris problem has been seen as only a long-term challenge for future generations. We believe that this is not true, but is instead also an immediate concern for space operations. A 2010 study investigates the cost of operating three different satellite constellations for 20 years [4] and shows that debris already causes significant cost for satellite operation today. The study concludes that in the most congested orbits, the cost of replacing satellites which go out of operation because of debris is increased between four and fourteen percent compared to a no-debris scenario. That translates into costs between seven hundred million and 1.4 billion US$ for each of the investigated satellite constellations over 20 years [4]. In addition, long-term projections show an exponential growth of the debris population over the next two centuries, even if no further space launches occur [5]. This increase is caused by collisions between debris and intact spacecraft and collisions between debris objects themselves. Both cases are sources for additional debris and drive a cascading effect, first described by Kessler [6]. Discussion on corrective measures mostly focuses on stabilizing the debris environment in the long-term by active debris removal (ADR) of four or five of the most massive objects per year, in order to remove sources of new debris. Monte-Carlo simulations have shown that this approach would stabilize the number of debris in Low Earth Orbit (LEO) [7]. However, those space missions will be costly and there will be no measurable immediate short term effect on collision risk, as the debris flux in LEO would remain virtually unchanged. Removing 5 out of 16,000 objects will not have a measurable impact on the overall risk of collision and it does not provide a short term capability to stop impending collisions.

The LightForce concept has considerable advantages. LightForce aims to reduce the risk of collisions by targeting conjunctions on warning (something ADR cannot do), and because LightForce is a ground-based technology, annual costs will be orders of magnitude lower. By tackling high risk conjunctions it addresses potential collisions directly. Taking part in stabilizing the debris environment (by preventing additional collision debris) is a secondary benefit. LightForce would use tracking data and orbit prediction to continuously compile and update a list of high risk conjunctions to engage. As illustrated in Fig.1, photon pressure from ground-based lasers would be used to alter the in-track velocity of space objects. Over time, that translates to an in-track displacement. Earlier research has shown that even if analysis is restricted to currently available industrial lasers, the approach has the potential to impact a significant fraction (several tens of percent) of conjunctions [25].

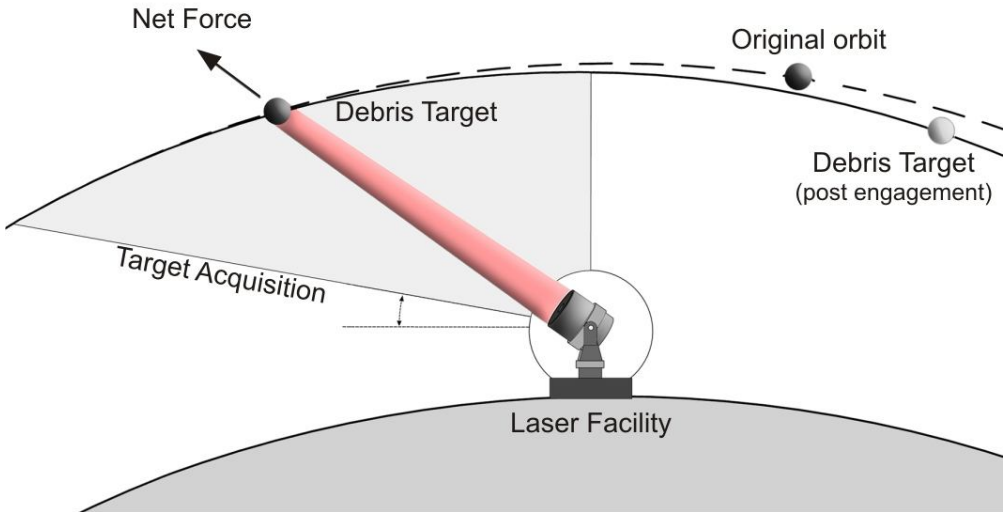

Fig.1: Schematic view of a laser facility and the operations for nudging space debris using photon pressure. Slowing down the debris results in loss of orbital energy, hence a lower orbit with a higher velocity. In general, both acceleration or deceleration can be useful to avoid a collision.

In an operational setting, LightForce would engage objects involved in a conjunction and simultaneously (and continuously) update orbital data. The goal of the presented research is to improve insight into how efficient LightForce is in reducing the risk of collisions in today's space environment.

This paper is divided into five parts. After this introduction (section 1), we outline our simulation approach (2), including the motivation for changes to our past approach. We then present the software implementation (3) on the NASA Ames Pleiades supercomputer and the resulting computing performance. Section 4 includes the results of several case studies, followed by a conclusion (5).

2. UPDATED SIMULATION APPROACH TO ASSESS LIGHTFORCE EFFICIENCY

2.1 Motivation for the updates

In the presented analysis we aim to deliver an improved benchmark for the LightForce space debris collision avoidance scheme for space operations, based on today's debris environment. Our past simulation approach [25] created a representative orbital environment of all tracked objects in Low Earth Orbit and then produced a list of all conjunctions with probabilities of collision (PoC, or P_c) larger than 10^{-6} for the given simulation time frame. For each conjunction in that list, the change in PoC that LightForce engagements could provide was calculated, providing a second list of conjunctions with different PoC. The overall efficiency was assessed by comparing the two lists. The restriction to 30 days was due to the need for high precision orbit simulations of approximately 15,000 objects on a single processor computer system. While this assessment investigated about two and a half thousand conjunctions, most of them are low probability (fig. 2).

As a result, it is uncertain how representative those results are in regard to high probability conjunctions with PoC>10^{-3}. Also, changing the orbital environment with LightForce engagement introduces the possibility of follow up conjunctions. New conjunctions with other objects were not assessed, as each conjunction in the list was assessed independently from all other objects. As LightForce introduces only minor changes to the orbits, the orbital environment does not change per se, and a worsening of the overall situation is not expected. However, the simulation approach from paper [25] cannot substantiate that statement. Hence we decided to expand our simulation effort to broaden the dataset and simulate the entire LEO environment continuously, and compare the situation with and without a simulated active network of LightForce ground stations. The computational requirements led to a decision to port the simulation to NASA Ames' massively parallel supercomputer system. The underlying physics of the simulation approach and the software implementation are described in section 3. The following section 2.2 describes the overall simulation approach.

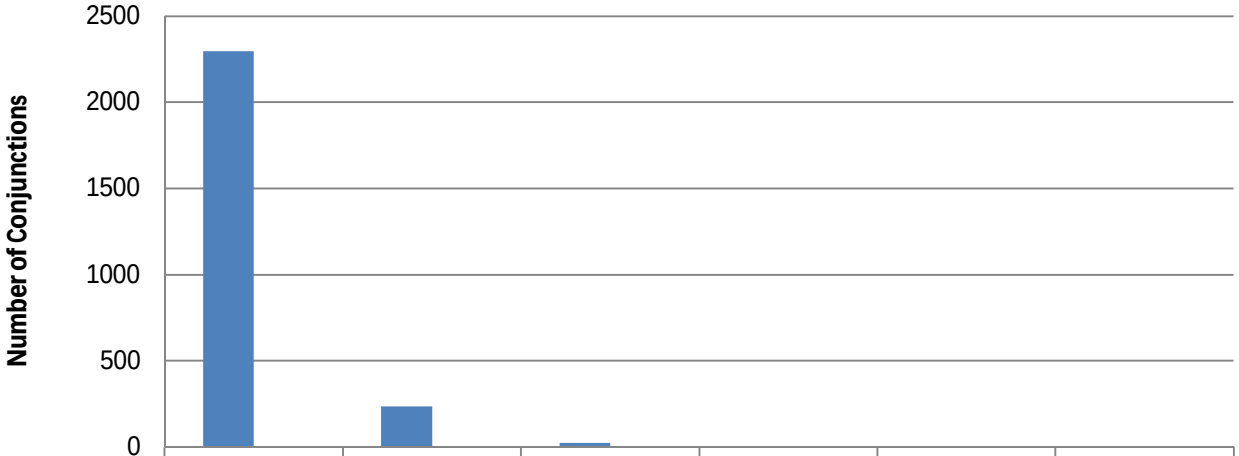

	10^{-6}<Pc<10^{-5}	10^{-5}<Pc<10^{-4}	10^{-4}<Pc<10^{-3}	10^{-3} <Pc<10^{-2}	10^{-2}<Pc<10^{-1}	10^{-1}<Pc<1
Occurence	2298	236	24	2	1	0
%	89.73	9.22	0.94	0.08	0.04	0.00

Fig.2: Distribution of conjunctions with maximum probability of collision P_c>10^{-6} detected over a 30 day period (June 15 to July 15, 2012, from [25])

2.2 Steps of the analysis

We analyze the probability of collision for all tracked space objects with and without an active LightForce system. The analysis follows three steps:

1) Create a baseline simulation (without LightForce). We utilize the publicly available two-line element (TLE) orbital data from the Joint Space Operations Center (JSpOC) to simulate the entire LEO environment and create a list of conjunctions that naturally occur during the simulated timeframe.
2) Simulate an active LightForce system. We propagate the same objects as in step 1, now including additional forces caused by an active LightForce system. All occurring conjunctions are recorded.
3) Assess the efficiency of the LightForce system. Both the list of naturally occurring conjunctions and the list of conjunctions with a LightForce system are compared using different metrics (Section 3).

In the following, we describe the three steps in more detail.

Step 1: Create a baseline (without LightForce)

As original input, we use the publicly available catalog of TLEs [9]. For each object the catalog provides a unique identifier and the orbital elements at a given epoch. Unfortunately, the catalogue does not directly provide an area-to-mass ratio. Also, single TLEs are error prone and have limited accuracy. To enable the best possible results (with reasonable efforts), we use least-squares fitting of TLE data as described by Levit and Marshall [1] to obtain an improved state vector, an area-to-mass ratio and a covariance uncertainty matrix. Details are described in the analogue section in last year's paper [25].

The algorithm results in an object database consisting of state vectors, area-to-mass-ratios and object areas. During the time interval chosen for our simulations[1] the catalog was made up of about 15,000 objects consisting of both active spacecraft and space debris. About 12,235 of the objects were in LEO with a perigee altitude below 2,000 km. There are about 500 active satellites in LEO.

Using the state vectors derived in step 1, we now propagate the orbits of the objects throughout the simulation time-frame and perform an all-on-all conjunction assessment. This gives us a sample of conjunctions based on real world data. If P_c for a given conjunction exceeds a threshold T_c, we save the data (object IDs, time of closest approach (TCA), P_c) in a list of high risk conjunctions.

Step 2: Simulate an active LightForce system

In the real world, a LightForce system will provide collision avoidance based on conjunction alerts. The accuracy of those alerts degrades over time due to inaccuracy of propagators. One illustrative reason for that inaccuracy is that orbits depend on the incoming radiation pressure from the sun, which is fluctuating and difficult to predict. Hence, the data created in Step 1 should not be misinterpreted for an attempt to predict conjunctions a year in advance, but as a way to create a representative baseline, using real world inputs. For space operations, tracking is used to continuously update the orbital data and collision avoidance decisions are made short term. LightForce would be used in a similar fashion, reacting to incoming tracking data from various sources, including high accuracy laser ranging data provided by the LightForce stations themselves. Hence, we do not attempt to develop an optimal engagement strategy for the entire simulation duration, but optimize that engagement strategy for a shorter time frame (e.g. one week) and continuously update that strategy. Figure 3 illustrates that approach.

The first step is a "search run", where we propagate the objects without LightForce for a given time frame (e.g. 9 days in advance, see fig 3). Occurring conjunctions are detected and an engagement strategy is developed using the following conditions, described in more detail in [25]:

A laser ground station will be tasked to illuminate an object, if all of the following apply:

a) There is a line of sight between the object and the laser and the elevation angle is >10 degrees.
b) The time remaining to the time of closest approach for the specific conjunction is less than a set engagement time t_e.
c) Laser activation is beneficial for the chosen optimal collision avoidance strategy, which is either to slow the object down, or to accelerate it.

[1] All our simulations used TLE's issued between June and December 2012.

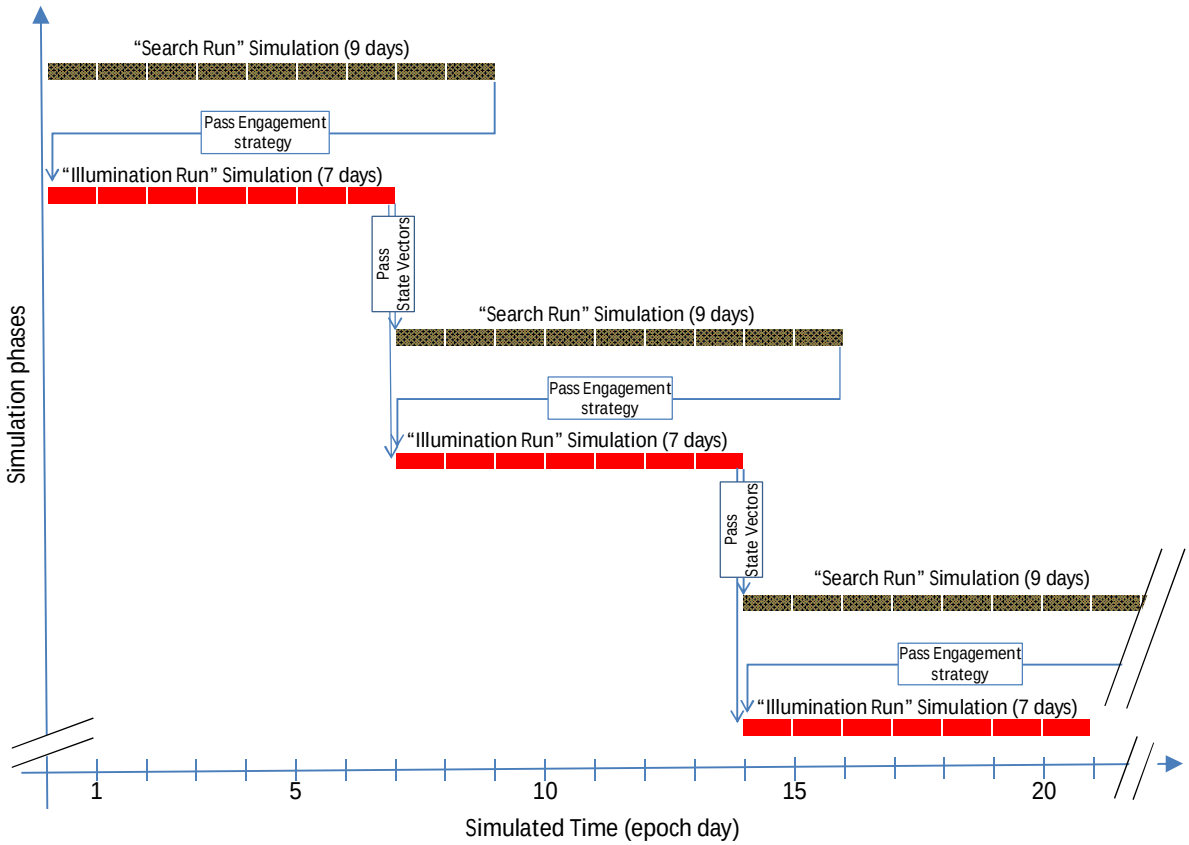

Fig.3: Simulation Phases. Search runs are used to develop the engagement strategy (decide when to turn on LightForce). Illumination runs are used to record conjunction data and assess the LightForce efficiency

At the end of the search run the software switches over to simulate LightForce engagements, to an "illumination run". Starting at day one, the engagement strategy from the first search run is now applied (e.g one week, red in fig 3). If a LightForce station is tasked to illuminate an object, the additional photon pressure derived force is added to the propagator. The illumination either happens during the first or second half of a pass, depending on whether accelerating or decelerating the object is more beneficial in reducing the PoC. All conjunctions and their final PoC are recorded throughout an illumination run. The state vectors of the objects at the end of the illumination run are input for the next pair of search and illumination runs. For the follow up search run, LightForce is turned off and a new illumination strategy is devised. The updated strategy is used for the follow on illumination run (fig. 3) which is a seamless continuation of the first illumination run, just with an updated illumination strategy that accounts for the changed environment. For the remainder of the simulation duration, search runs and illumination runs are alternating, simulating a LightForce system that reacts to incoming updated tracking data.

The duration of a search run is that of an illumination run plus the engagement time t_e, in order to allocate t_e of potential illumination time for each conjunction. For example, fig. 3 illustrates a 9 day search run followed by a 7 day illumination run, in order to allow for 48 hours of engagement time for each conjunction. This way, LightForce will engage a conjunction that occurs at the beginning of the second illumination run during the end of the first illumination run. Please note that the actual illumination time (where the debris is illuminated by the laser) will be much shorter than the engagement time, as each pass over a ground station lasts only a few minutes. The choice of a two day engagement time and seven day illumination runs was made in order to assess a basic system. Optimizing the strategy towards an ideal system is by no means trivial and would also require in depth simulation of the interaction of the existing tracking systems with the additional high precision laser tracking data provided by the LightForce system. That simulation would require a range of assumptions about the capabilities of existing and future tracking networks, hence we choose not to go that route and stick with a basic 9 day / 7 day schedule.

We also implemented a more complicated version which allows for search runs with activated LightForce system in order to check for producing accidental conjunctions with LightForce. If that option is used, search runs with and without LightForce are used to devise an optimized engagement strategy.

It is important to understand that while the computer is alternating between simulations that are used to either develop an engagement strategy or simulations used to test it, the final illumination runs are continuously using the same state vectors over the entire simulation duration (1 year), and record the final PoC of each occurring conjunction. These combined illumination runs build up a one year simulation of an active LightForce system. The results of that run are compared to the baseline in the next step.

Step 3: Assess the efficiency of the LightForce system

We compare the baseline list of conjunctions to the list from combined illumination runs (LightForce is active). As in [25], we use two different metrics, the mitigation factor *M* and the reduction factor *R*:

The mitigation factor *M* is defined as

$$M = 1 - \frac{\text{Number of conjunctions with } P_c > T_c \text{ after LightForce activation}}{\text{Number of conjunctions with } P_c > T_c \text{ without LightForce}} \quad . \tag{2}$$

M can be derived directly from the simulation data when a reasonable threshold T_c is set. M answers the question what fraction *M* of conjunctions can a LightForce system mitigate, meaning, what fraction of high risk conjunctions can be mitigated to low risk conjunctions. This is useful for an operator who wants to know what fraction of conjunctions LightForce can mitigate.

The reduction factor *R* is defined as:

$$R = 1 - \frac{\sum_{\text{all conjunctions with } P_c > T_c \text{ after LightForce activation}} P_c}{\sum_{\text{all conjunctions with } P_c > T_c \text{ without LightForce}} P_c} \quad . \tag{3}$$

R provides an assessment on the overall effect of a LightForce system on the debris environment, comparing the sum of P_c with a Lightforce system to the sum of P_c without. The sum of P_c represents the expected value of the number of collisions caused by the assessed conjunctions with $P_c > T_c$ during the simulation time frame. Hence, the parameter *R* represents the reduction of the expected value of number of collisions for the case when LightForce is activated, compared to the situation when it is not. More details on *R* can be found in [25]

3. SOFTWARE IMPLEMENTATION AND PERFORMANCE ON PARALLEL SYSTEM

3.1 Software implementation on a highly parallel system

Physics and Astrodynamics implementation

The implemented propagator, including the calculation of the photon pressure, and the calculation of the probability of collision P_c follow the approach described in [25]. For completeness, we summarize the relevant sections from [25]. Significant changes are implemented for the all-on-all conjunction analysis scheme and the software architecture, described at the end of this section.

Propagator

The scheme used by the propagator for the numerical integration is a 4th/5th order Runge-Kutta scheme with variable time step [12,13]. The forces taken into account during the propagation include Earth's gravitational field, the gravitational perturbations from the Moon and the Sun, atmospheric drag and the solar radiation pressure. The numerical implementation is built around the NAIF SPICE Toolkit [14] and the physical model used for each force is referenced in Table 1. We validated our propagator against STK's HPOP, an industry standard.

Laser induced photon pressure
Laser illumination entails four additional force components. Three of them are caused by conservation of photon momentum (photon pressure), a fourth is induced by temperature gradients in the surface of the illuminated object. The first force component is parallel to the incoming laser beam and caused by the momentum of all incoming photons. This is the most significant force component. Specular reflected photons add an additional force parallel to their outgoing direction (but with a negative sign). Diffuse reflection adds another force. Finally, temperature gradients on the surface could result in a net force through thermally emitted photons. However, surface reflectivities, as well as object orientation are not very well known for most of the objects. In addition, most objects over 600 km are assumed to be tumbling fast, which would result in cancelling the latter three effects for most cases [19]. Even if the object is not tumbling, the influence is comparably minor. Hence we ignore those additional effects and go with the conservative assumption of a debris object with zero reflectivity for the analysis presented in this paper.

Under this assumption, the additional force F on the object is [20]

$$F(t) = \frac{1}{c}\int I(x,y,t)dA\,, \tag{1}$$

where c is the speed of light, I is the irradiance at a point on the cross-section of the illuminated object at the time t. We update the irradiance for each time step. The irradiance I is calculated taking multiple effects into account. These effects are beam spread by diffraction, beam spread by atmospheric turbulence, and power losses by atmospheric absorption and scattering. All depend on the specific path between the laser ground station and the space object (determining distance and atmospheric conditions) and the technical specifications of the stations.

Table 2 in Section 4 (simulation results) summarizes those specifications. We assume a ground station with adaptive optics and a laser guide star to compensate some of the effects of turbulence. As assumption for the performance of the adaptive optics system we use the results of 1998 benchmark experiments on an adaptive optics system for a directed energy weapon system, compiled in a study of the American Physical Society [21]. Combining the different effects result in the irradiance and the force on the object. The details of the calculations are complex, please see references [2,3,22] and references therein for a step-by-step description.

Calculate Probability of Collision
We follow the method described by Patera [18]. For each conjunction we determine both the real and the maximum probability of collision [10, §11.7.2]. The real probability of collision takes into account the covariance determined by the initial TLE fit in step 1, while the maximum probability of collision is a value obtained by varying the orientation and the size of the uncertainty ellipsoid defined by that covariance. To be on the safe side, we evaluate the performance of the laser photon pressure against the maximum probability of collision for subsequent calculations. It is the maximum probability of collision we commonly denote as P_c.

Software architecture & All on All conjunction analysis
The All-on-All conjunction analysis was significantly updated since last year's paper [25]. The main incentive for that was the shift to a highly parallel approach in order to utilize the Pleiades supercomputer at NASA Ames. Pleiades is a Linux cluster made of Intel Xeon processors. Our current software is implemented in C and uses the standard Message Passing Interface (MPI) for parallelization.

Table 1: Forces taken into account in the dynamical modeling of the debris and the models used for their numerical implementation.

Force	Numerical implementation	Reference
Earth's Gravitational Field	Earth Gravitational Model 1996 (EGM96)	[15]
Luni-Solar Perturbations	NASA JPL Planetary Ephemerides	[16]
Atmospheric Drag	NRL-MSISE-00 model	[17]
Solar Radiation Pressure	Debris modeled as a sphere, eclipses taken into account	[10]
Laser Radiation Pressure	In-house model	[2]

After initialization, the code produces a time series of state vectors using the high precision propagator. This is called "heavyweight propagation". The propagator generates “anchor” points for each space object for whatever times it sees fit. No attempt is made to restrict or encumber the propagator's decisions, other than to stop after a fixed number of points are generated. The propagator is allowed to just "run free", producing a new position/velocity point for an object whenever it felt it was appropriate to maintain the specified error tolerance. This is done fully in parallel, with each MPI rank doing heavyweight propagation on a subset of the objects, and then exchanging the results with the other ranks. When complete, each MPI rank has the full set of information about every object.

With the anchor points in hand, each MPI rank interpolates the position of all objects for the beginning of the current time step, starting from the anchor points. This is called "lightweight propagation". This is simple and fast, and for the comparatively small number of objects being considered (12,235) it is actually slower to try and do this in parallel (the overhead is higher than the potential gain). These positions are then sorted along the X-axis.

The code next does collision detection. Each MPI rank assigns itself a subset of the objects, and decides if an object might possibly interact with some other object during the current time step. Ultimately, this determination is made by calculating the time of closest approach, which determines whether a conjunction occurs in the current time step. The calculation of the time of closest approach is computationally expensive. Hence, the code goes to great lengths to try and prove that two objects could not possibly have interacted during the time step, and so avoid the call if possible. If a conjunction occurs, at the TCA for a pair of objects the associated state and co-state information is used to calculate the probability of collision and the conjunction is recorded.

After the current time step is complete, we advance the clock and lightweight propagate to the beginning of the next time step. If we no longer have enough time series information to reach the end of the next time step, we first do another round of heavyweight propagation to get the needed anchor points, and then use lightweight propagation. The cycle continues until the simulation is complete. The physics of applying LightForce (or not) is handled in the propagator.

A primary concern in this work was producing consistent answers. Since the propagator uses the current state as the basis for predicting the next state, even very tiny differences are quickly magnified, and after a few days an object could be many kilometers away from the position predicted by some previous run. Neither is better or more correct than the other, and both will probably produce very similar statistics. But it is not easy to compare the two directly. Great effort was expended to make it at least possible to avoid this sort of problem. For example, the code may save the state vectors at any time and then later restart from reading that file. This gives bitwise identical results compared to running the simulation straight through.

3.2 Software Performance

As of August 2014, the Pleiades supercomputer consists of a total of 184,800 cores, distributed over a mix of the following types of Intel Xeon processors: E5-2680v2 (Ivy Bridge), E5-2670 (Sandy Bridge), and X5670 (Westmere). The system is an SGI ICE cluster connected with InfiniBand in a dual-plane hypercube technology. The simulation architecture described in this paper scales well up to 1000 cores, which is the maximum we used. Propagating 12,235 objects for 365 days using the scheme from Fig. 3 takes approximately 4 hours. This is 52 nine-day segments (the search run, without LightForce), plus 52 seven-day segments (the illumination run, with LightForce). This adds up to a total of just under 20,000 hours of simulation time and a performance of approximately 5000 times real time.

4. SIMULATION RESULTS FOR UPDATED EFFICIENCY ANALYSIS

4.1 Input parameters

In the following we present our current simulation results on the efficiency of a network of LightForce ground stations for space debris collision avoidance. The presented case uses a set of parameters which are introduced in this section.

For the orbit propagation, we used the force models summarized in Table 1. The start date of our simulation was June 15, 2012 (a random choice) and 5 TLEs for fitting were acquired before that date. The resulting state vector was computed for June 15 at 00:00:00 UTC. We restricted the analysis to orbits with a perigee below 2000 km.

To compile the baseline list of conjunctions, we performed the previously described all-on-all conjunction analysis with a threshold T_c of 10^{-6} because it appears to be the standard value at which major international space players,

commercial and institutional, start to get interested in the PoC metric. Actual collision avoidance maneuvers (using satellite maneuvers) will not be initialized until P_c is orders of magnitude higher [23].

The input parameters for the laser force model are stated in Table 2, translating to commercial off-the-shelf technology where possible, to cut down the cost of a potential system. For the same reason, assumptions about the adaptive optics technology are based on 1998 benchmarks [2, 3, 22]. The engagement time t_e is 48h, meaning that LightForce begins engaging objects 48 hours before the TCA for a specific conjunction. In this paper, we always assume a set of four stations with 20 kW laser output power, placed at the locations specified in table 2a.

As explained in [25], we do not constrain our analysis to certain sun illumination conditions, but assume a laser engagement for each pass over a ground station in compliance with the requirements of Section 2-2 step 2.

The engagement strategy is updated on a weekly basis, using the state vectors at the end of a seven day illumination run and propagating for nine days (as in fig. 3). We choose to implement a double optimization cycle, propagating a first search run without LightForce and then another one with LightForce to ensure to capture potential secondary conjunctions. The simulation duration was one year.

There is still room for further optimization. As a simulation runs approximately 5000 faster than real time, in a operational scenario one would likely update the engagement strategy whenever new tracking data is available and not in seven day cycles.

Table 2: Laser ground station parameters used for efficiency simulations

Laser	IPG YLS-10000-SM	Telescope diameter	1.5 m
Power	20 kW continuous	Atmosphere model	US Standard 1976
Wavelength	1070 nm	Aerosol model	MODTRAN rural (VIS=23 km)
Beam quality	M^2=1.3	Turbulence model	Hufnagel/Valley 5/7
Engagement time t_e*	48 h	Adaptive optics	performance according to [21], Fig.21.1; additional beam degradation by tip/tilt anisoplanatism, see[21], appx. D4.4

* Each object is engaged while passing over a ground station in a 48 h window before the time of closest approach of the specific conjunction.

Table 2a: Laser ground station locations for efficiency simulations

Location	**Latitude**	**Longitude**	**Altitude [km]**
Antarctica (Ant.)	-80.4	77.4	4.1
Hawaii (HI)	20.7	-156.3	3.0
Australia (Aus.)	-35.3	149.0	0.8
Alaska (AK)	64.9	-148.5	0.5

4.2 Simulation Results

Baseline

The first step to assessing LightForce is to create a baseline that will be compared to the results with an active LightForce system. The data was extracted from a simulation spanning from June 15 2012 to June 14, 2013. The distribution of detected conjunctions with $P_c > 10^{-6}$ is broken down into a histogram with P_c intervals (fig. 4). In comparison to the data from the one month period [25] (fig. 2), the total number of conjunctions increased by a factor of 11.6 and the relative distribution between the P_c intervals remains very similar. There is a 4% decrease of propagated objects over 12 months. That decrease is caused by natural decay of objects into the atmosphere. In reality, the number is actually increasing due to satellite launches and fragmentation debris, but we did not add a source term to the simulation described in this paper. As both the baseline and the LightForce simulation use the same assumption, we do not expect any significant impact to the efficiency metrics presented.

1 year result with LightForce activated

As the next step, we assess a simulation with active LightForce stations, record the remaining conjunctions with $P_c > 10^{-6}$ and compare them to the baseline. Fig. 5 shows the effect of the defined 4 station LightForce network (Antarctica, HI, Aus, AK, see Table 2a) with a 20 kW laser each in a histogram view. It shows the distribution of the number of conjunctions over the defined P_c intervals.

The total number of conjunctions with $P_c > 10^{-6}$ is decreased by 85%, resulting in an overall mitigation factor M=85% (as defined in section 2.2). Fig. 6 shows the mitigation factor M, for each of the P_c intervals defined in fig. 5. The remaining conjunctions are mostly naturally occurring conjunctions but also include conjunctions that appear because the whole space environment is changing due to LightForce application to some of the objects. However, it is obvious that the overall effect to the environment is positive.

This result is reinforced by assessing the cumulative P_c for all occurring conjunctions. Fig. 7 shows the increase of cumulative P_c over time, comparing the baseline case with the LightForce case. The observed steps occur when high risk conjunctions are detected. The cumulative increase is less with LightForce active, translating into a reduced number of expected collisions. The overall reduction factor R (see section 2.2) for the entire simulation duration is 94% (counting conjunctions with $P_c < 10^{-6}$ as zero), including all conjunctions that occur in the modified debris environment. Compared to the result in [25], that is an increase of 5%.

Finally, fig. 8 shows the influence of the simulation duration on the calculated M and R factors. Both stabilize with increased simulation duration. M shows less variation than R, as high risk and low risk conjunctions are weighed equally for M. High risk conjunctions dominate the R factor. As there are fewer of those, it takes more time for R to stabilize. Nevertheless the results are stable for the second half of the 12 months simulation duration.

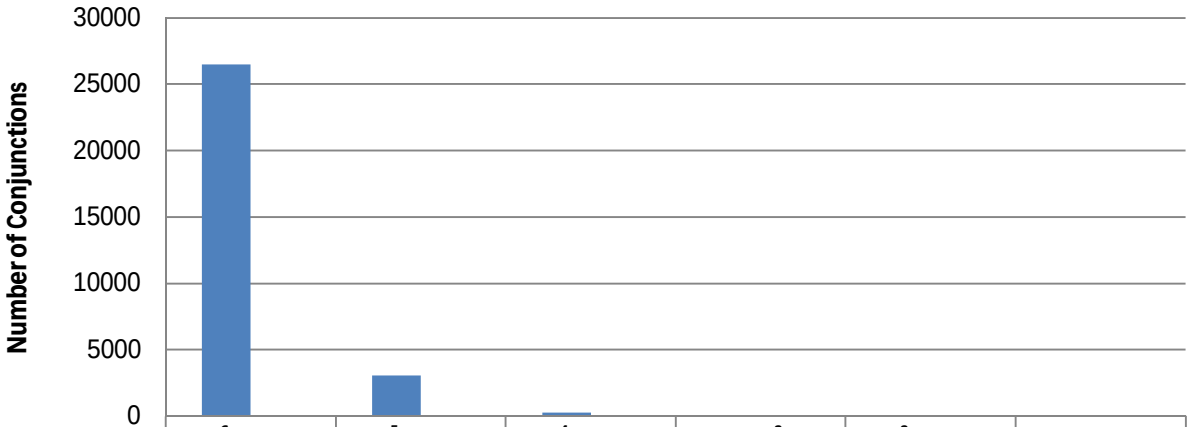

	$10^{-6}<Pc<10^{-5}$	$10^{-5}<Pc<10^{-4}$	$10^{-4}<Pc<10^{-3}$	$10^{-3}<Pc<10^{-2}$	$10^{-2}<Pc<10^{-1}$	$10^{-1}<Pc<1$
Occurence	26479	3073	290	34	4	0
%	88.62	10.28	0.97	0.11	0.01	0.00

Fig.4: Distribution of conjunctions with maximum probability of collision $P_c > 10^{-6}$ detected over a 52 week period

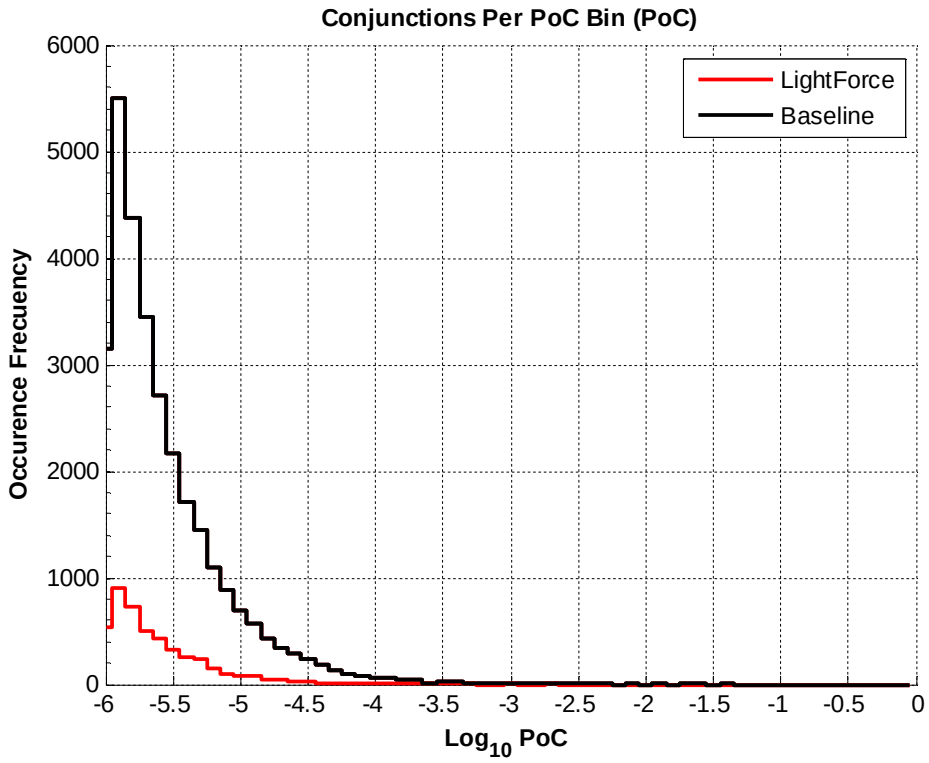

Fig.5: Histogram of the distribution of conjunctions with $P_c > 10^{-6}$ detected over a 52 week period. *: Baseline:* without LightForce. *LightForce:* Remaining conjunctions while 4 20kW LightForce stations are active. Each interval is defined as $10^{-6+0.1*n} < P_c < 10^{-6+0.1*n+1}$; starting with the interval $10^{-6} < P_c < 10^{-5.9}$ and increasing.

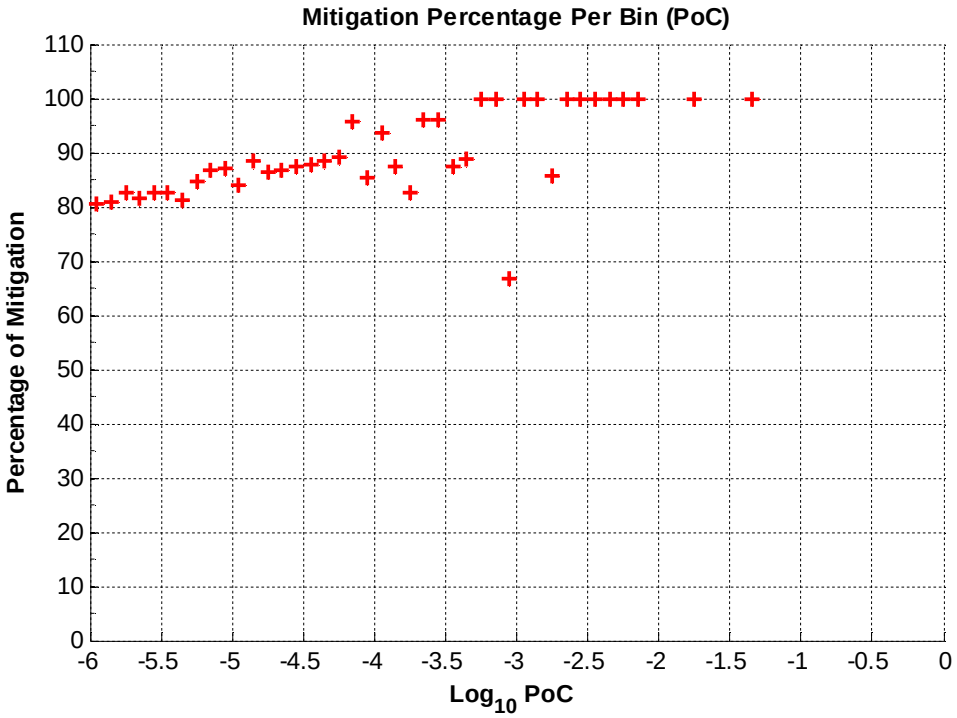

Fig.6: Mitigation factor M assessed for conjunctions sorted by P_c. Each point in the plot represents a calculation of M for all conjunctions that originally appear within a $10^{-6+0.1*n} < P_c < 10^{-6+0.1*n+1}$ interval, starting with the interval $10^{-6} < P_c < 10^{-5.9}$ and increasing. Note: The underlying data gets sparse for $P_c > 10^{-3}$ (fig 4)

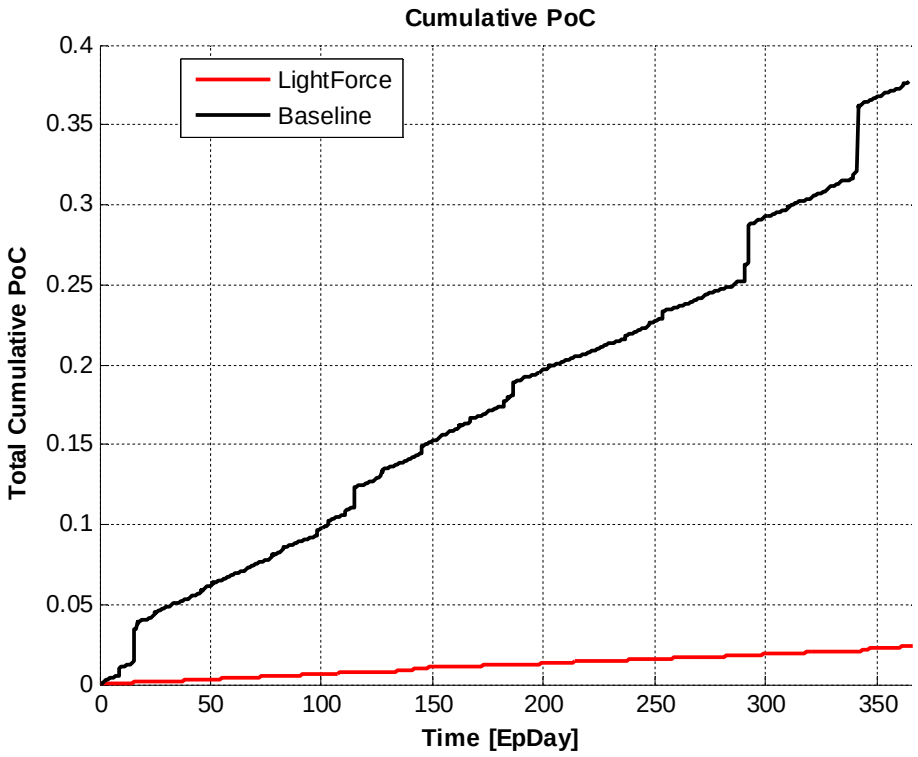

Fig.7: Cumulative P_c plotted over the duration of the simulation for both the baseline and the LightForce case.

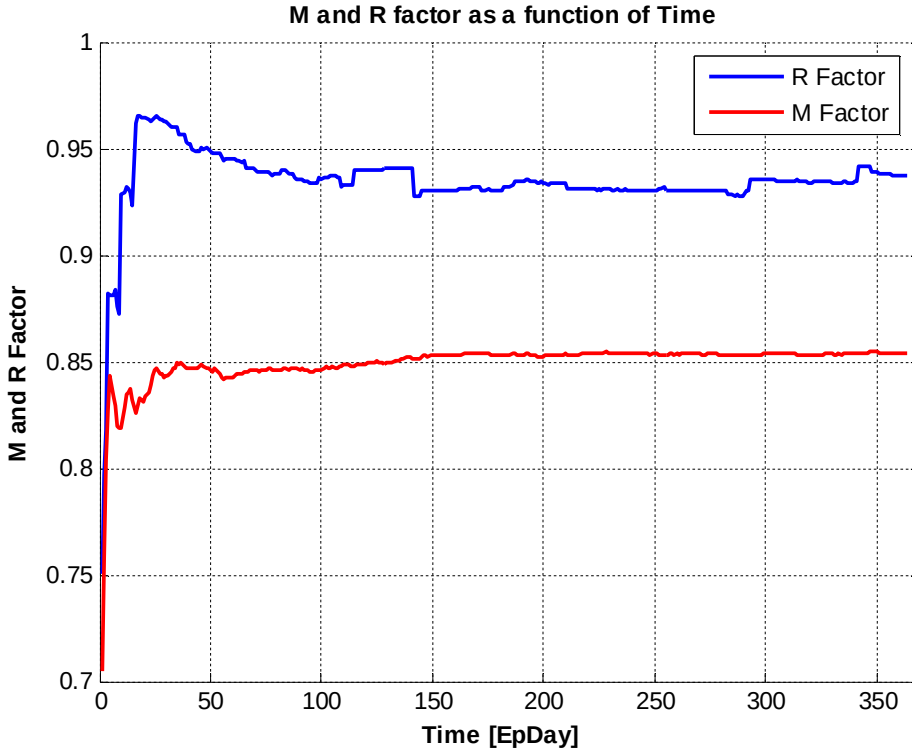

Fig.8: *M* and *R* factors depending on simulation duration. *M* is defined as the fraction of mitigated conjunctions; *R* is the reduction in expected number of collisions with cataloged objects.

5. CONCLUSION

We updated the efficiency analysis of the LightForce space debris collision avoidance system provided in [25]. This update utilizes a highly parallel simulation approach implemented on NASA Ames' Pleiades supercomputing cluster. The simulation approach enables an assessment roughly five thousand times faster than real time. This capability was utilized to simulate the entire LEO environment with and without LightForce interactions for an entire year. In order to take into account that the quality of orbit predictions rapidly deteriorates over a few days in the real world, no attempt to optimize the whole engagement strategy for the one year timeframe is made. Instead, the engagement strategy is updated on a weekly basis, simulating a reaction of the system to updated tracking data. The results are promising. Compared to the one month simulation duration presented in [25], both efficiency metrics have improved with the added data. Results indicate that utilizing a network of four stations with 20kW lasers, 85% of all conjunctions with $P_c>10^{-6}$ can be reduced to below $P_c<10^{-6}$. The reduction factor R is now over 90%, which indicates a significant reduction in expected number of collisions with space debris, should a LightForce system be implemented.

6. ACKNOWLEDGEMENTS

The authors would like to thank their colleagues and the center management at NASA Ames Research Center for continuing support. We also would like to thank our colleagues at Electro Optic Systems (Canberra, Australia), Lawrence Livermore National Laboratory and the Air Force Research Laboratory for useful discussions and their support.

7. REFERENCES

1. Levit, C. and Marshall,W. "Improved orbit predictions using two-line elements." *Advances in Space Research* Vol. 47 No.7 (2011): 1107-1115.
2. Mason, J.; Stupl J.; Marshall, W.; Levit, C. "Orbital debris–debris collision avoidance." *Advances in Space Research* Vol. 48 No. 10 (2011): 1643-1655.
3. Stupl, J.; Mason, J.; Marshall, W.; Levit, C.; Smith, C.; Olivier, S.; Pertica. A.; De Vries, W."LightForce: An Update on Orbital Collision Avoidance Using Photon Pressure." *63rd International Astronautical Congress*; Naples, Italy; 1-5 Oct. 2012; IAC-12.A6.5.11.p1.x14662.
4. Ailor, W.; Womack, J.; Peterson, G.; Lao, N." Effects of Space Debris on the Cost of Space Operation." *61st International Astronautical Congress*; Prague; Czech Republic, 29. Sept-1 Oct. 2010; IAC-10.A6.2.10, 7p.
5. Liou, J.-C. and Johnson, N. "Instability of the present LEO satellite populations." *Adv. Space Res.*, 41, 1046-1053, 2008.
6. Kessler, D. and Cour-Palais, B. "Collision frequency of artificial satellites: The creation of a debris belt." *J. of Geophys.* Res., 83(A6), 2637–2646, 1978.
7. Liou, J.-C. and Johnson, N.L., Hill, N.M. "Controlling the growth of future LEO debris populations with active debris removal." *Acta Astronautica* 66(2010), 648--653.
8. Wiedemann, C.; Flegel, S.; Möckel, M.; Gelhaus, J.; Braun, V.; Kebschull, C.; Kreisel, J.; Metz, M.; Vörsmann, P. "Cost Estimation of Active Debris Removal". *63rd International Astronautical Congress*; Naples, Italy; 1-5 Oct. 2012; IAC-12.A6.5.3. Note: The paper estimates $140M, at the presentation the author mentioned that projections in the community range from $140M-$500M.
9. www.space-track.org
10. Vallado, D.A. "Fundamentals of Astrodynamics and Applications", New York 2007.
11. Barton, D.K; Brillinger, D.; El-Shaarawi, A.H.; McDaniel, P.; Pollock, K.H.; Tuley, M.Y. "Final Report of the Haystack Orbital Debris Data Review Panel", NASA Technical Memorandum 4809, Feb. 1998.
12. Dormand, J. R.; Prince, P. J. (1980), "A family of embedded Runge-Kutta formulae", *Journal of Computational and Applied Mathematics* 6 (1): 19–26
13. Hairer, E.; Nørsett, S.P.; Wanner, G. "Solving ordinary differential equations I: Non stiff problems." New York 2008.
14. Acton, C.H. "Ancillary data services of NASA's Navigation and Ancillary Information Facility." *Planetary and Space Science* 44.1 (1996): 65-70.

15. Lemoine, F.G.; Smith, D.E.; Kunz, L.; Smith, R.; Pavlis, E.C.; Pavlis, N.K.; Klosko, S.M.; Chinn, D.S.; Torrence, M.H.; Williamson, R.G.; Cox, C.M.; Rachlin, K.E.; Wang, Y.M.; Kenyon, S.C.; Salman, R.;Trimmer, R.; Rapp, R.H.; Nerem, R.S."The development of the NASA GSFC and NIMA joint geopotential model." *Gravity, Geoid and Marine Geodesy*, International Association of Geodesy Symposia Nr 117 (1997): 461-469.
16. Folkner, W.M.; Williams, J.G.; Boggs, D.H. "The planetary and lunar ephemeris DE 421." IPN Progress Report (2008): 42-178. http://tmo.jpl.nasa.gov/progress_report/42-178/178C.pdf
17. Picone, J. M.; Hedin, A.E; Drob, D.P.; Aikin, A.C. "NRLMSISE-00 empirical model of the atmosphere: Statistical comparisons and scientific issues." *Journal of Geophysical Research: Space Physics* (1978–2012) 107.A12 (2002): SIA-15.
18. Patera, R.P. "*General method for calculating satellite collision probability*." *Journal of Guidance, Control, and Dynamics* 24.4 (2001): 716-722.
19. Phipps, C.R.; Albrecht, G.; Friedman, H.; Gavel, D.; George, E.V.; Murray, J.; Ho, C.; Priedhorsky,W.; Michaelis, M.M. and Reilly, J.P. “ORION: Clearing near-Earth space debris using a 20-kW, 530-nm, Earth-based, repetitively pulsed laser.” *Laser and Particle Beams* 14 no.1 pp. 1–44, 1996.
20. McInnes, C.K. “Solar sailing: technology, dynamics, and mission applications.”Springer, 1999.
21. Barton, D. K.; Falcone, R.; Kleppner, D.; Lamb, F. K.; Lau, M.K.; Lynch, H. L.; Moncton, D.; Montague, D.; Mosher, D. E.; Priedhorsky, W.; Tigner, M. and Vaughan, D. R. “Report of the American Physical Society Study Group on Boost-Phase Intercept Systems for National Missile Defense: Scientic and Technical Issues.” *Reviews of Modern Physics* 76, No. 3, S1-, 2004. See Fig.21.1, p. S323.
22. Stupl, J. and Neuneck, G. “Assessment of Long Range Laser Weapon Engagements: The Case of the Airborne Laser.” *Science & Global Security* 18, no. 1 (2010): 1-60, see appendix A.
23. Laporte, F.; Moury, M.; Pena,X. “Operational experiences in Collision Avoidance for LEO satellites”, *ISU Symposium* (February 2009), http://forum2.isunet.edu/index2.php?option=com_docman&task=doc_view&gid=775&Itemid=26 .
24. Nikolaev, S.; Phillion, D.; Springer, H.K.; de Vries,W.; Jiang,M.; Pertica, A.; Henderson, J.; Horsley, M.; Olivier, S. “Brute Force Modeling of the Kessler Syndrome”, *AMOS 2012*.
25. Stupl, J.; Faber, N.; Foster, C.; Yang Yan, F.; Levit, C.; “LightForce Photon-Pressure Collision Avoidance: Efficiency Assessment on an Entire Catalogue of Space Debris”AMOS 2013,10-13 September 2013,Wailea, HI